SPE/ISRM 78170

Quantifying Rock Capillary Strength Behavior in Unconsolidated Sandstones

G. Han, SPE, M.B. Dusseault, SPE, University of Waterloo; J. Cook, SPE, Schlumberger Cambridge Research

This paper was prepared for presentation at the SPE/ISRM Rock Mechanics Conference held in Irving, Texas, 20-23 October 2002.

Abstract

Changes in water saturation or rock wettability can lead to rock instability and sand production. The effects of saturation on rock strength have two origins - chemical sensitivity and changes in capillary forces. In this paper, a detailed study of capillary rock strength behavior after water breakthrough is carried out for four different models. These four models account for particle-particle interactions and include spherical particles in tangential contact, differently sized spheres in tangential contact, squeezed contacts, and detached spheres. The effects of fluid properties (e.g. contact angle and surface tension), rock properties (e.g. particle size, size ratio, contact fabric), and deformation of loaded rock on capillary strength have been mathematically expressed and quantified.

The model calculations indicate:

- For all the models, capillary strength increases linearly with increasing surface tension between fluid phases.
- Contact angle influences both the magnitude of capillary strength and its variation with saturation. The larger the contact angle, the lower the magnitude (under the same water saturation) and the faster its decrease with increasing saturation.
- If the particle size is uniform, small particle size results in high capillary strength. If particles have different sizes, the size ratio of the particles has a similar influence on capillary strength as does fluid contact angle: it affects both the magnitude of capillary strength and its variation with water saturation. However, the relationships are different: the smaller the size difference, the higher the magnitude and the slower its decrease with saturation.
- For the detached and squeezed models the capillary force (or strength) firstly increases with water saturation, then decreases after a critical saturation, in contrast to the tangential contact model where capillary force always decreases with water saturation.
- Through the introduction of the strain concept into the capillary models, they can be used to describe capillary strength variations with rock deformation. It is found that capillary strength more-or-less reaches a maximum when spheres are tangentially contacted, and decreases in both the squeezed and detached states, but decreasing much faster with increasing deformation in the squeezed state.

These improvements in the micromechanical modeling of sands will be used to build our understanding of sand production in very weak or unconsolidated rocks, clarifying how sand production is affected by changes in saturation.

Introduction

Extensive experiments have been carried out to study the effect of water saturation (or moisture content, humidity, etc.) on the strength and elastic properties of shale[1,2], chalk[3,4,5], and sandstone[1,6,7,8,9,10,11]. In summary, those experiments found that:

- Strength reduction with increased saturation is generally found for all rock samples, with a strength reduction of from 8%[6] to 98%[7], depending on rock texture, mineralogy, fluid chemistry, etc.;
- Most of the strength decrease occurs after only a slight increase of water saturation (or moisture content) from the dry state[6,7,12]. Further increases in moisture content have little effect on rock strength and properties;
- The value of the friction coefficient appeared to remain unaltered in many cases[1,11,13], but some researchers[4,14] found it varies with water saturation (up to 10° [4]) if the rock surface chemically reacted with water, thus causing a change in the surface smoothness; and,
- Young's modulus decreases with water content increases, sharing the same trend as rock strength. Poisson's ratio may increase or decrease slightly before a general increase takes place[6,15] at higher saturations.

Many hypotheses and models have been put forward to rationally explain these capillarity phenomena, such as:[18]

- Chemical reactions between water and rock solids, e.g. quartz hydrolysis, carbonate dissolution, ferrugineous deposition in the direction of lowering rock strength, and other Rebinder effects;

- Changes of capillary force with water saturation;
- Higher fluid pressure gradients, therefore higher fluid velocities and drag forces in the presence of two phase flow;
- Blockage of pore throats by interstitial fragments or particles mobilized because of the fluid flow; and,
- Shale swelling that leads to a locally increasing pressure gradient and destabilizing force.

Furthermore there may be several mechanisms acting at the same time, each contributing to rock instability. Since about 70% oil comes from unconsolidated or weakly consolidated sand[16], and, on average, oil companies today produce three barrels of water for each barrel of oil[17], understanding and quantifying the mechanisms leading to sand instability in two-phase (water and oil) fluid flow conditions in unconsolidated reservoirs become important engineering goals. However, quantifying all these mechanisms is a substantial challenge under current research conditions[18].

In this paper, we focus on capillarity in unconsolidated (uncemented) siliceous sand. The capillary effects are created by liquid menisci between sand particles, which affect rock mechanical behavior. Four different models are proposed to describe capillary strength under different fabric states.

Model Development

Considering practical possibilities in developing analytical or semi-analytical models in particulate systems, the following contact fabrics are studied: uniform particles contacting tangentially[18], non-uniform particles, uniform detached particles, and uniform squeezed particles. Each model is developed in a similar manner.

Tangentially Contacting Non-Uniform Particles.

Basic Scheme. Fig. 1 illustrates the situation of two non-uniform sand particles contacting tangentially. Assuming that the shape of the liquid bridge is a toroid characterized by radii r and r_1, a commonly accepted formula to calculate capillary pressure cross the liquid water bridge has been developed:

$$\Delta P = \gamma\left(\frac{1}{r_1} - \frac{1}{r}\right) \quad \text{.....(1)}$$

The precision of the toroid approximation is within 10% of the value obtained by numerical solution of the Laplace-Young equation[19].

The Pressure Difference Method is used to calculate capillary cohesive force resulting from capillary pressure since it is demonstrated to be more reasonable[18]:

$$F_{ci} = \pi x_i^{\,2} \Delta p \quad \text{.....(2)}$$

where i is 1 or 2, and F_{c1}, F_{c2} are the capillary forces exerted on the interfaces between particle 1 and the liquid bridge, and between particle 2 and the liquid bridge, respectively. Since the capillary bond always breaks at its weakest point, the smaller of the two capillary forces, i.e. $\overline{F_c} = F_{c2}$, should be used in the following equation[20, 21, 22]:

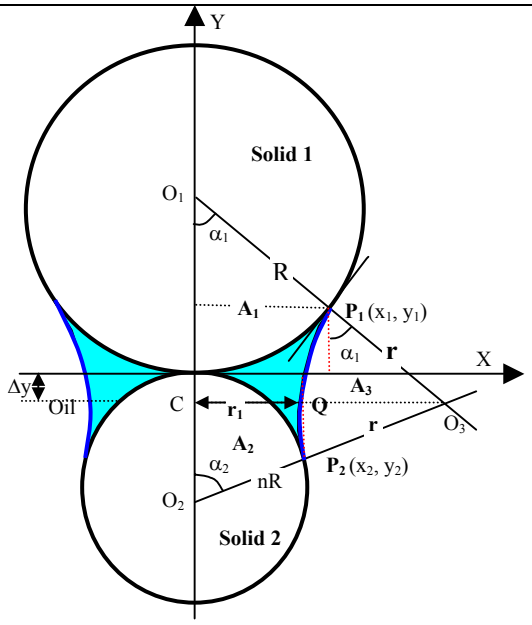

Fig. 1: Model for non-uniform particles

$$\sigma_T = \lambda \frac{1-\phi}{\phi} \frac{F_{c2}}{4\overline{R}^2} \quad \text{.....(3)}$$

where $\overline{R} = (R + nR)/2$, and λ is a factor accounting for non-uniform particle sizes effects on total rock strength[22]. A value of λ = 6~8 is suggested for packs of particles with a narrow size range, and λ=1.9~14.5 for packs with wider particle size distributions. Therefore, based on a Mohr-Coulomb strength criterion, the UCS can be approximately expressed as [18]

$$\sigma_{UCS} = \lambda \frac{1-\phi}{\phi} \frac{\sin\varphi}{1-\sin\varphi} \frac{F_c}{2\overline{R}^2} \quad \text{.....(4)}$$

which illustrates that, for unconsolidated sand, rock strength is related to rock porosity, friction angle, capillary force, particle size, and size distribution.

Geometrical Expressions for Model Parameters. Assuming the contact angle θ = 0, for solid 1 in Fig.1, the coordinates of contact point P_1 are

$$x_1 = R\sin\alpha_1;\ y_1 = R(1-\cos\alpha_1) \quad \text{.....(5)}$$

and those of contact point P_2 for solid 2 are

$$x_2 = nR\sin\alpha_2;\ y_2 = nR(1-\cos\alpha_2) \quad \text{.....(6)}$$

In triangle O_1O_3C, the distance between x-axis and point O_3 is

$$\Delta y = (R + r)\cos\alpha_1 - R \quad \text{.....(7)}$$

comparing with

$$\Delta y = nR - (nR + r)\cos\alpha_2 \quad \text{.....(8)}$$

established from triangle O_1O_2C. Therefore the relation of r, α_1, and α_2 can be determined as

$$(n+1)R = (R + r)\cos\alpha_1 + (nR + r)\cos\alpha_2 \quad \text{.....(9)}$$

Based on the cosine rule for triangle $O_1O_2O_3$, the liquid bridge radius r can be expressed as a function of α_1:

$$r = \frac{1-\cos\alpha_1}{\cos\alpha_1 - \frac{1-n}{1+n}} \cdot R \quad \text{.....(10)}$$

Substituting r of Eq.(10) into Eq.(9), the relationship between two water volume angles (α_1, α_2) can be determined:

$$\cos\alpha_2 = \frac{(n^2+1)\cos\alpha_1 + (n^2-1)}{(n^2-1)\cos\alpha_1 + (n^2+1)} \quad \text{.....(11)}$$

In order to determine capillary pressure from Eq.(1), the other radius (r_1) of the liquid bridge must be specified. Neither x_1 nor x_2 is suitable since the capillary pressure should be uniform inside the liquid bridge. In this model, the point Q (see Fig.1) is selected as a "median" point of the bridge, while its x coordinate,

$$r_1 = (R + r)\sin\alpha_1 - r \quad \text{.....(12)}$$

serves as an expression of its "median" radius.

The water volume in the unit cell (Fig.2) is equal to the water saturation volume, i.e. $V\phi S_w$, where $V\phi$ is the porous volume of the unit:

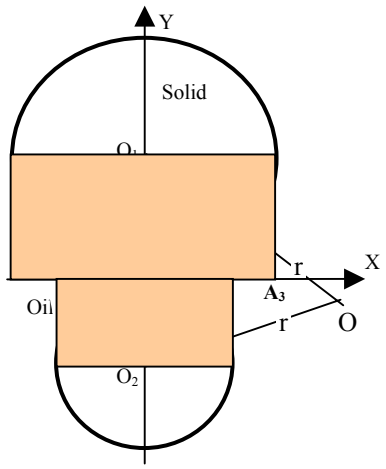

Fig.2: Definition of unit volume

$$V\phi = 2(1 - \frac{\pi}{4}) \cdot (1 + n^2)R^2 \quad \text{.....(13)}$$

Therefore

$$V\phi S_w = (n+1)(r+R)R\sin\alpha_1 - (\alpha_1 + \alpha_2 n^2)R^2 - (\pi - \alpha_1 - \alpha_2)r^2 \quad \text{.....(14)}$$

where r and α_2 can be expressed in terms of α_1 through Eq.(10) and Eq.(11). Consequently, for any value of water saturation, the liquid bridge radii (r, r_1) can be explicitly determined by Eq. (12, 14), and the capillary force and capillary strength can therefore be determined explicitly.

Tangentially Contacting Uniform Particles. Following the same development steps as above, when particles are uniformly sized, i.e. size ratio n = 0, and the contact angle (θ) is not zero, the expressions for bridge radii become

$$r = \frac{1-\cos\alpha_1}{\cos\alpha_1} \cdot R \quad \text{.....(15)}$$

and

$$r_1 = x_p - r + r\sin(\theta + \alpha) \quad \text{.....(16)}$$

where $x_p = R\sin\alpha$. The expression for water saturation becomes

$$\phi \cdot S_w = -\frac{\alpha}{2} + \sin\alpha - \frac{1}{4}\sin 2\alpha - \frac{(1-\cos\alpha)^2}{1+\cos 2(\alpha+\theta)} \cdot \left[\frac{\pi}{2} - (\alpha+\theta) - \frac{\sin 2(\alpha+\theta)}{2}\right] \quad \text{.....(17)}$$

Thereby for any water saturation, capillary pressure can be

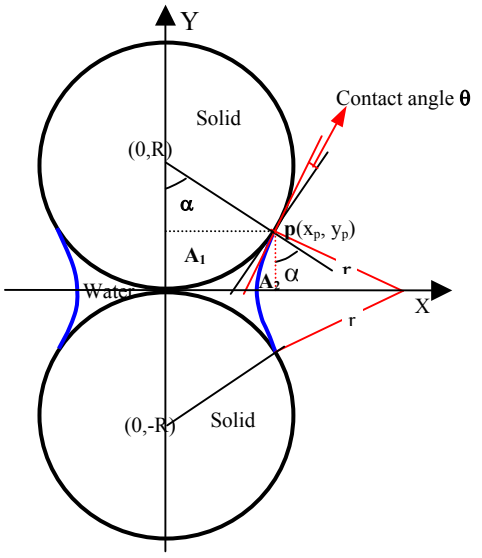

Fig.3: Model for uniform particle contacting tangentially

determined by Eq.(1).

Since there is no particle size difference, the capillary force can be determined easily as

$$F_c = \pi x_p^{\,2} \Delta p \quad \text{.....(18)}$$

and the capillary strength therefore becomes

$$\sigma_T = \frac{1-\phi}{\phi}\frac{F_c}{4R^2} \quad \text{.....(19)}$$

Detached Uniform Particles. Besides tangential contacts, there are several other contact fabrics that may exist between particles in a granular geological medium, such as floating, sutured, convex-concave, and long contacts[23]. Figs. 4 and 5 summarize this classification into two possible microscopic cases: uniform particles are detached from each other (which may be an artifact of the sampling and preparation procedure); or they are compressionally squeezed and overlap to form convex-concave or long contacts.

For the detached case (Fig. 4), the expression for the radius r can be written as[24]

$$r = \frac{1+k-\cos\alpha}{\cos(\alpha+\theta)}\cdot R \quad \text{.....(20)}$$

where k is the ratio of the half distance between particles to the particle radius (i.e. k = a/R). The water saturation becomes

$$(1+k)\left[1-\frac{\pi}{4(1+k)}\right]S_w = -\frac{\alpha}{2}+(1+k)\sin\alpha-\frac{1}{4}\sin 2\alpha-$$

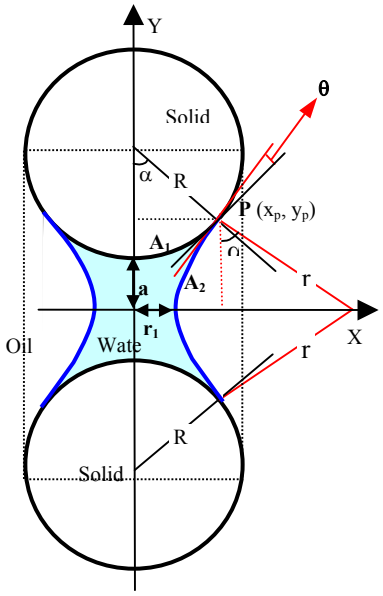

Fig. 4: Models for detached particles (a > 0)

$$\left[\frac{1+k-\cos\alpha}{\cos(\alpha+\theta)}\right]^2\cdot\left[\frac{\pi}{4}-\frac{\alpha+\theta}{2}-\frac{1}{4}\sin 2(\alpha+\theta)\right] \quad \text{.....(21)}$$

When the contact angle θ = 0, this equation can be simplified:

$$(1+k)\left[1-\frac{\pi}{4(1+k)}\right]S_w = -\frac{\pi}{4}+(1+k)\sin\alpha-$$
$$\left(\frac{\pi}{4}-\frac{\alpha}{2}-\frac{1}{4}\sin 2\alpha\right)\left[\left(\frac{1+k}{\cos\alpha}\right)^2-\frac{2(1+k)}{\cos\alpha}\right] \quad \text{.....(22)}$$

Combining Eq. (16), (20), (21) and Eq. (1), (18), (19), the capillary strength can again be determined.

Squeezed Uniform Particles. For the case of squeezed particles (i.e. a < 0, Fig. 5), the angle β is introduced to describe the extent of the compressive squeezing, compared to the water volume angle α. It can be determined by[24]

$$\beta = \arccos(1-k) \quad \text{.....(23)}$$

Similarly, the other parameters used to calculate capillary strength can be solved:

$$r = \frac{1-k-\cos\alpha}{\cos(\alpha+\theta)}\cdot R \quad \text{.....(24)}$$

and

$$(1-k)\left[1-\frac{\pi-2\beta+\sin 2\beta}{4(1-k)}\right]S_w = \frac{-\alpha+\beta}{2}+(1-k)\sin\alpha-\frac{1}{4}(\sin 2\alpha+$$
$$\sin 2\beta)-\left[\frac{1-k-\cos\alpha}{\cos(\alpha+\theta)}\right]^2\cdot\left[\frac{\pi}{4}-\frac{\alpha+\theta}{2}-\frac{1}{4}\sin 2(\alpha+\theta)\right]$$
$$\text{.....(25)}$$

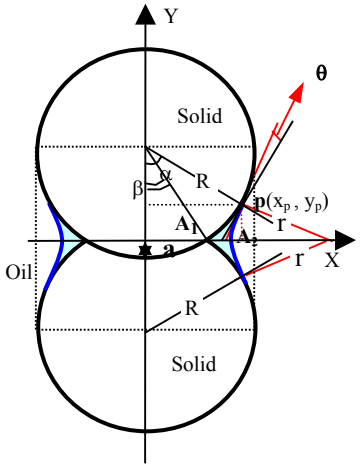

Fig. 5: Models for squeezed particles (a < 0)

If the contact angle θ = 0, the above equation becomes

$$(1-k)\left[1-\frac{\pi-2\beta+\sin 2\beta}{4(1-k)}\right]S_w=\frac{-\alpha+\beta}{2}+(1-k)\sin\alpha-\frac{1}{4}(\sin 2\alpha+\sin 2\beta)-\left[\frac{1-k-\cos\alpha}{\cos\alpha}\right]^2\cdot\left[\frac{\pi}{4}-\frac{\alpha}{2}-\frac{1}{4}\sin 2\alpha\right] \quad \text{.....(26)}$$

Combining Eq. (16), (24), (25) and Eq. (1), (18), (19), the capillary strength can be expressed as a function of water saturation, particle radius, contact angle, and the degree of compressive squeezing.

Loading of Uniform Particles. In Fig. 4 and Fig. 5, the volumetric deformation of the particles can be expressed as

$$\varepsilon=\frac{\Delta V}{V}=\frac{2R(2R+2a)-2R\cdot 2R}{2R\cdot 2R}=\frac{a}{R} \quad \text{.....(27)}$$

Coincidently, it is equal to k, the ratio of the half distance between particles to the particle radius. Therefore the models developed above for detached and squeezed particles can be used to describe the variations of capillary strength with rock deformation, except that, instead of the water saturation, water volume in the liquid bridge between particles should remain constant. The water volume in the liquid bridge for the detached particle state can be calculated by

$$Q_w=4R^2(1+k-\frac{\pi}{4})\cdot S_w \quad \text{.....(28)}$$

whereas for the compressed case it is:

$$Q_w=4R^2\left[(1-k)(1-\frac{1}{2}\sin\beta)-\frac{\pi}{4}+\frac{1}{2}\beta\right]\cdot S_w \quad \text{.....(29)}$$

Models Verification and Discussion

The parameters used in the following discussions are listed in Table 1, unless otherwise specified. This parameter list shows the inherent simplicity of the models: only particle radius, surface tension, contact angle, porosity, and friction angle are needed to estimate the magnitude of capillary strength.

Table 1. Parameters used in the models

R (m)	γ (N/m)	ϕ (%)	φ (°)	θ
0.0002	0.036	30	60	0

Model Simplifications. Compared to the models developed elsewhere[18,24], the models presented here can be used to analytically describe the behaviors of capillary strength under different rock, fluid, and loading conditions. Some assumptions made during the model development should be clearly restated, such as:

- The liquid bridge formed between particles can be described as a toroid;
- The variable bond strength between particles can be replaced by a mean value that is applicable throughout the whole rockmass;
- The water content is distributed evenly inside the particulate rock mass; and,
- The particles deform elastically upon compressive loading (squeezing).

Whereas these may be viewed as limitations to the models' applicability, we believe that because the models capture the essential physics, adjustments and calibration can easily be incorporated so as to give useful results in practice.

Factors Influencing the Capillary Strength. Besides water saturation, there are many factors that can affect capillary strength. They can be categorized into three types: fluid properties (e.g. surface tension and contact angle), rock properties (e.g. particle size, size distribution, contact fabric), and external loading condition (extension or compression).

Contact Angle. Based on the model developed above, the effect of contact angle between fluid and rock on the variations of capillary strength with water saturation is calculated and plotted in Fig. 7. It is shown that contact angle not only affects the magnitude of capillary strength (capillary force decreases with an increase of contact angle), but also affects its decrease rate with water saturation (the bigger the angle, the faster the decrease). However, at any saturation there is no significant difference of the magnitude of capillary forces when the angle changes from 0 to 0.2.

Surface Tension. Fig. 8 illustrates the simulated relation of capillary strength to surface tension between wetting and non-wetting fluids under different water saturations (0.5%, 3.3%, 9.5%). It is found that rock strength is positively propotional to the surface tension, and its increase rate becomes slower when water saturation rises.

Particle Size. Particle size has significant impact on rock capillary strength, as shown in Fig. 9: strength increases dramatically (up to 10 kPa) when particle size decreases below some critical value (around R = 0.15 mm), even though model calculations indicate that the capillary force actually decreases when particles becomes small. The main reason for this rather dramatic effect is that the interactions among rock particles rather than the fluid-rock interactions become the dominant factor determining rock strength: the finer the sand particles, the higher the rock strength. Since the radii of sand particles in oil-producing formations are usually 60 to 400 μm, the magnitude of rock strength resulting from capillary forces can be expected to be as high as the range of several kPa.

Size Difference. Fig. 10 shows the effect of non-uniform size on capillary strength, noting that λ in Eq.(4) is set as a constant (λ = 8). The size ratio of the particles has a similar influence on capillary strength as does the fluid contact angle: it affects both the magnitude of capillary strength and its variation rate with water saturation. But the relations are

different: the smaller the size difference, the higher the capillary strength and the faster its decrease. Furthermore, at the same water saturation (1%), a smaller difference in particle sizes (i.e. higher value of n) leads to greater values for the capillary force and strength, even though the capillary pressure does not increase after reaching a maximum value when the size ratio n is around 0.5 (Fig. 11). The reason for different trends of capillary pressure and capillary force is that the force (or strength) not only depends on pressure, but also on the area being acted upon. When the area increase overwhelms the pressure decrease, their product, the capillary force, will mainly track the area changes.

Contact Fabric. Figs. 12 and 13 demonstrate the relations between capillary strength and water saturation for detached and compressed particles, respectively. Compared to tangentially contacting particles (k = 0 in the figures), where the strength continuously decreases with water saturation, when particles are separated or compressed ($k \neq 0$), capillary strength will not reach its peak until some critical water saturation. Furthermore, the greater the distance between particles, either positive (detached) or negative (squeezed), the higher the water saturation that is needed to attain the maximum capillary strength. This is reasonable because there will be more water needed for widely spaced particles to form a strong liquid bridge than for more closely spaced particles.

Strength Evolution with Rock Deformation. A character of capillary force is that it does not break abruptly with rock deformation. This means that before the sands deform to the extent that grains are fully disaggregated, the capillary force still exists during the progressive weakening, dilation and separation processes.

Fig. 14 illustrates variations of capillary tensile strength when rock is deformed. Following the conventions of rock mechanics, a negative sign for deformation means extension, whereas a positive sign means compression. Interestingly, when water volume in the liquid bridge is constant, the tensile strength resulting from capillary forces keeps decreasing with rock compression, whereas it increases slightly with extensional deformation before beginning to continuously decrease with strain. This difference becomes more obvious when there is more water in the bridge, as demonstrated by the curve of $Q_w = 6.87\times10^{-9}$ m^3 in Fig. 14.

Moreover, the decrease rate of the capillary strength under compression is much faster than that under extension. In reservoir situations, the intact reservoir sand inevitably has to experience compression due to the increases in effective stress during reservoir depletion, and in these conditions, the capillary strength may decrease rapidly with water saturation. On the other hand, if rock has experienced considerable compaction beforehand and particles are originally in a squeezed state when oil production starts, the capillary strength can be expected to be relatively small, depending on the degree of compaction.

Model Verifications.

Tangential Contacts Model. It has been demonstrated[18] that the model for tangentially contacted uniform particles can fit the experiment data[25] very well. Based on tests of a medium to fine-grained sandstone (Waterstone, UK) poorly cemented with clay, Dyke and Dobereiner[7] developed a relation between rock strength and moisture content (Fig. 6), and found that most strength reduction occurs within a limited moisture content range (1%). The model cacluations agree with their experimental results: in Fig. 7, capillary strength clearly decreases rapidly with water saturation after water saturation increases to a specific value. Furthermore, this specific value is closely related to contact angle (Fig. 7), size ratio between particles (Fig. 10), and contact fabric (Figs. 12 & 13).

Detached or Squeezed Model. Experiments with unconsolidated sand[16] show that a stable arch starts to develop even with a small increase in water saturation ($S_w > 3\%$) in a two-phase environment, whereas such an arch cannot be stable in a monophasic condition. Furthermore, the sand starts to flow into the wellbore when $S_w > 20\%$, and massive sand production occurs if $S_w > 32\%$. The models developed for detached and squeezed particles (Fig. 12, Fig. 13) can explain these phenomena directly: the strength from capillary force first increases to a peak value (therefore sand arches form) before continuously decreasing and disappearing as water saturation increases (hence the sand arches collapse).

Strength Evolution Model. Because of the difficulty of executing laboratory experiments under the challenging conditions of no external confining stress in a granular medium, in the petroleum industry there is as yet no experimental data available to confirm the evolution of capillary strength with rock deformation. However there are some experiments reported in the chemical engineering literature that show the effect of detached distance on capillary force. For example, Fig. 15 contains experimental results from Mason and Clark[26]. The spheres used are oil-wetted and water-immersed, with radii of 15 mm. Each curve corresponds to a constant water volume in the liquid bridge, and it generally decreases with the separation distance shortly after a slight increase, which is the same as the curves with negative k in Fig. 14.

Conclusions

Four different models are developed and verified to account for the variations and behaviors of rock strength resulting from capillary forces in two-phase fluid environments, including spherical particles in tangential contact, differently-sized spheres in tangential contact, squeezed and detached spheres. The effects of fluid properties (contact angle and surface tension), rock properties (particle size, size ratio, contact fabric), and deformation of loaded rock on capillary strength have been mathematically expressed and quantified.

The model calculations indicate:

- Capillary strength generally decreases with water saturation and eventually disappears after some specific water saturation. This specific value is affected by contact angle, size difference between particles, and contact fabrics.
- Capillary strength increases linearly with increasing surface tension, and its increase rate becomes slower at higher water saturation.
- Contact angle influences both the magnitude of capillary strength and its variation with saturation. The larger contact angle leads to a lower strength and a faster decrease rate with increasing saturation.
- Smaller particles result in higher capillary strengths.
- When particles have difference sizes, the smaller size ratio (i.e. the larger size difference) results in lower capillary strengths and slower decreases with saturation.
- For detached and squeezed particles, the capillary strength first increases with water saturation, then decreases after a critical saturation, in contrast to the tangential contact model, where capillary forces continuously decreases with water saturation.

The models developed can be used for describing the variations of capillary strength with rock deformation. It is found that, when water volume in the liquid bridge is constant, the strength keeps decreasing with rock compression, whereas it increases slightly with extensional deformation before continuously decreasing. Furthermore capillary strength decreases much faster when particles are squeezed.

Acknowledgement

The authors thank Dr. Denis Heliot, and Dr. Steve Chang from Schlumberger for having initiated the studies. The technical communications with Dr. Luis C.B. Bianco from PetroBras are deeply appreciated.

Nomenclature

a = *half distance between two particles, m*
F_c = *capillary force, N*
k = *ratio of half distance between particles to particle radius*
n = *size ratio (the ratio of two particles radii)*
ΔP = *capillary pressure, Pa*
Q_w = *water volume in the liquid bridge, m^3*
r_1 = *radius of curvature of the liquid bridge in the horizontal plane, m*
r = *radius of curvature of the liquid bridge in the vertical plane, m*
R = *radius of the particles, m*
S_w = *water saturation, fractional (1.0 = 100% water saturation)*
UCS = *uniaxial (unconfined) compressive strength, Pa*
x_p, y_p = *the spatial coordinates of point P(x,y), m*
α = *water volume angle, degree*
β = *angle to describe squeezed extent, degree*
ε = *strain, dimensionless*
θ = *contact angle between fluid and solid, radian*
γ = *surface tension between two fluids, N/m*
ϕ = *porosity of the defined unit, dimensionless*
φ = *friction angle defined in a linear Mohr-Coulomb yield criterion*
σ_T = *tensile strength of rock, Pa*

References

1. Colback, P.S.B. and Wild, B.L.: "The Influence of Moisture Content on the Compressive Strength of Rocks", Proceedings of 3rd Canadian Symposium of Rock Mechanics, 65-83, 1965.
2. Forsans, T.M., and Schmitt, L.: "Capillary Force: the Neglected Factor in Shale Stability", Proc. Eurock'94, 71-84, Delft, 1994.
3. Papmichos, E., Brignoli, M., and Santarelli, F.J.: "An Experimental and Theoretical Study of a Partially Saturated Collapsed Rock", Mechanics of Cohesive-Frictional Materials, 2, 251-278, 1997.
4. Gutierrez, M., Øino, L.E., and Høeg, K.: "The Effect of Fluid Content on the Mechanical Behaviour of Fractures in Chalk", Rock Mechanics and Rock Engineering, 33 (2), 93-117, 2000.
5. Brignoli, M., Santarelli, F.J., and Righetti, C., "Capillary Phenomena in an Impure Chalk", Eurock '94, 837-843, Balkema, Rotterdam, 1994.
6. Hawkins, A.B. and McConnell, B.J.: "Sensitivity of Sandstone Strength and Deformability to Changes in Moisture Content", Quarterly Journal of Engineering Geology, 25, 115-130, 1992.
7. Dyke, C.G., and Dobereiner, L.: "Evaluating the Strength and Deformability of Sandstones", Quarterly Journal of Engineering Geology, 24, 123-134, 1991.
8. Bruno, M.S., Bovberg, C.A. and Meyer, R.F.: "Some Influences of Saturation and Fluid Flow on Sand Production: Laboratory and Discrete Element Model Investigations", the 1996 Annual Technical Conference and Exhibition, Denver, Colorado, 1996.
9. Dube, A.K. and Singh, B: "Effect of Humidity on Tensile Strength of Sandstone", J. Mines, Metals and Fuels, 20-1, 8-10, Jan.1972.
10. Boretti-Onyszkiewicz, W.: "Joints in the Flysch Sandstones on the Ground of Strength Examinations", Proc. 1st Cong. Int. Soc. Rock Mech., 1, 153-157, Lisbon, 1966.
11. Skjærstein A., Tronvoll, J., Santarelli, F.J. and Jøranson, H.: "Effect of Water Breakthrough on Sand Production: Experimental and Field Evidence", SPE 38806, SPE Annual Technical Conference and Exhibition, San Antonio, TX, Oct. 1997.
12. West, G.: "Effect of Suction on the Strength of Rock", Quarterly Journal of Engineering Geology, 27, 51-56, 1994.
13. Swolfs, H.S.: "Chemical Effects of Pore Fluids on Rock Properties", Underground Waste Management and Environmental Implications, Proc. Symp. American Association of Petroleum Geologists (AAPG), Memoir 18, 224-233, Dec.6-9, 1971.
14. Horn, H.M., and Deere, D.W.: "Frictional Characteristics of Minerals", Geotechnique, 12, 319-335, 1962.
15. Priest, S.D. and Selvakumar, S.: "The Failure Characteristics of Selected British Rocks", Transport and Road Research Laboratory Report, 1982.
16. Bianco, L.C.B., and Halleck, P.M.: "Mechanisms of Arch Instability and Sand Production in Two-Phase Saturated Poorly Consolidated Sandstones", SPE 68932, the SPE European Formation Damage conference, Hague, Netherlands, May 2001.
17. Bailey, B., Crabtree, M., Tyrie, J., Kuchuk, F., Romano, C. and Roodhart, L.: "Water Control", Oil Field Review, 30-50, 2000.

18. Han, G., and Dusseault, M.B.: "Quantitative Analysis of Mechanisms for Water-Related Sand Production", SPE 73737, the SPE International Symposium and Exhibition on Formation Damage Control held in Lafayette, LA, U.S.A., Feb. 2002.
19. Lian, G., Thornton, C. and Adams, M.J.: "Effect of Liquid Bridge Forces on Agglomerate Collisions", Powders & Grains, 59-64, 1993.
20. Schubert, H.: "Tensile Strength of Agglomerates", Powder Technology, 11, 107-119, 1975.
21. Capes, C.E.: "Particle Size Enlargement", Handbook of Powder Technology, 1, 23-26, 1980.
22. Schubert, H.: "Capillary Forces – Modelling and Application in Particulate Technology", Powder Tech., 47, 105-116, 1984.
23. Taylor, J.M.: "Pore Space Reduction in Sandstone", Bull. Am. Assoc. Pet. Geol., 34, 701-716, 1950.
24. Han, G., and Dusseault, M.B.: "Strength Variations with Deformation in Unconsolidated Rock after Water Breakthrough", SCA 2002-22, Proceedings of the 2002 Symposium of SCA (Society of Core Analysis), Monterey, CA, U.S.A., Sept. 2002.
25. Tremblay, B., Oldakowski, K. and Settari, A.: "Geomechanical Properties of Oil Sands at Low Effective Stress", 48th Ann. Tech. Meeting of the Petro. Soc., Calgary, Alberta, Jun. 1997.
26. Mason, G., and Clark, W.C.: "Liquid Bridges between Spheres", Chem. Eng. Sci., 20, 859, 1965.

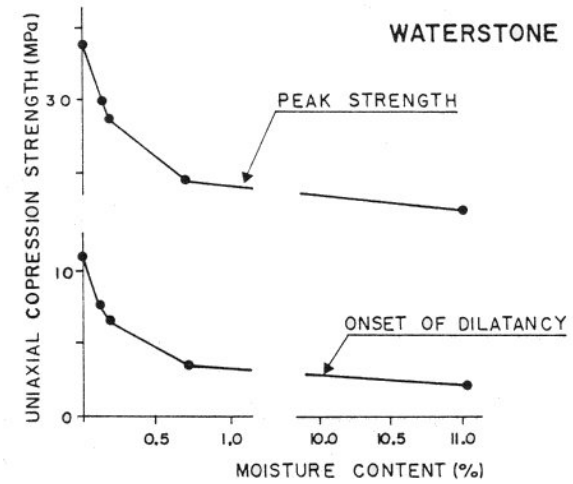

Fig.6: Variations of rock strength with water saturation
(After Dyke and Dobereiner[7])

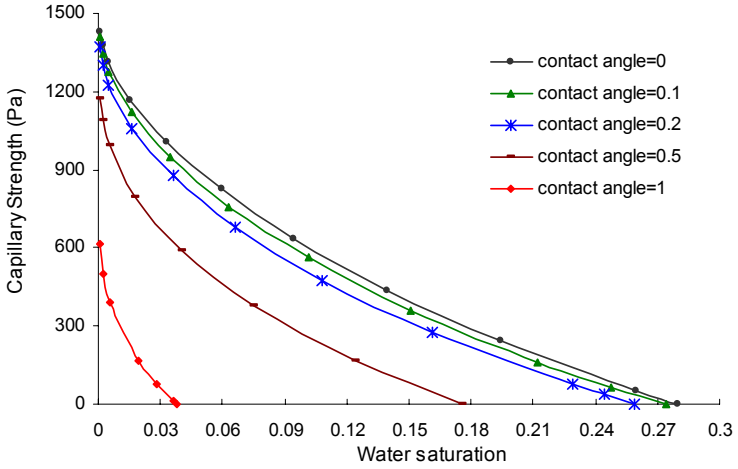

Fig.7: Capillary strength (UCS) vs. contact angle

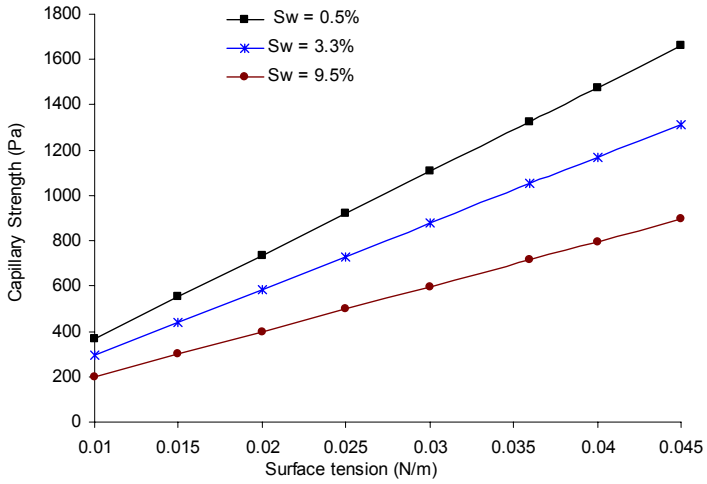

Fig.8: Capillary strength (UCS) vs. surface tension

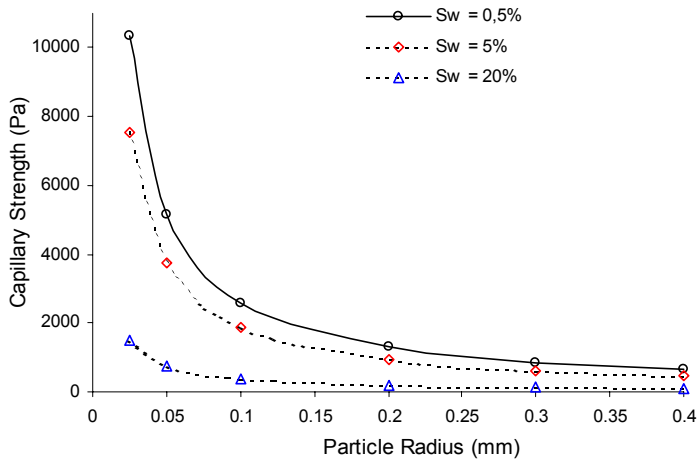

Fig.9: Capillary strength (UCS) vs. particle size

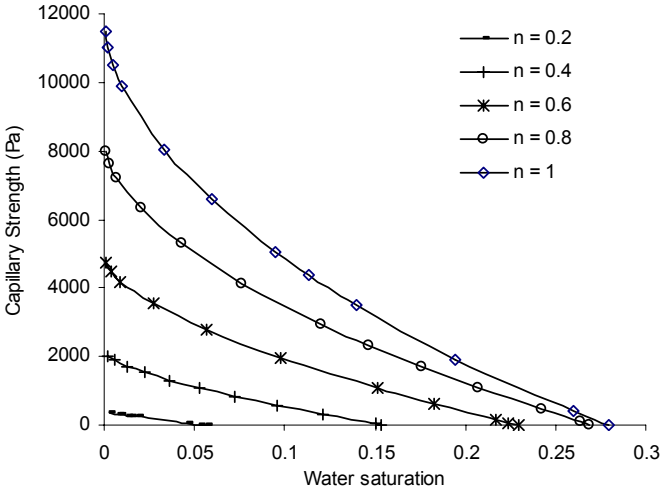

Fig.10: Capillary strength (UCS) at different size ratios

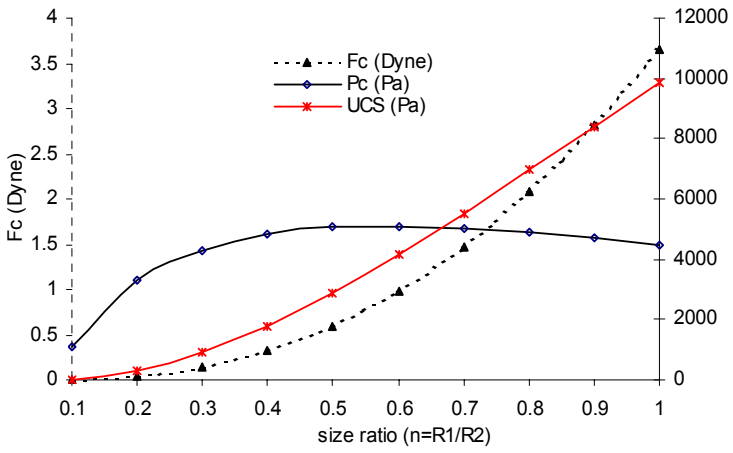

Fig.11: Capillary strength (UCS) vs. size ratio (S_w =1%)

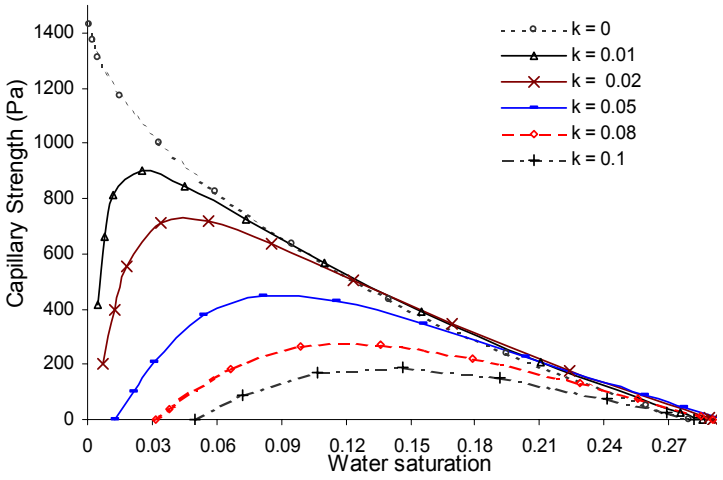

Fig.12: Variations of capillary strength (UCS) in detached state

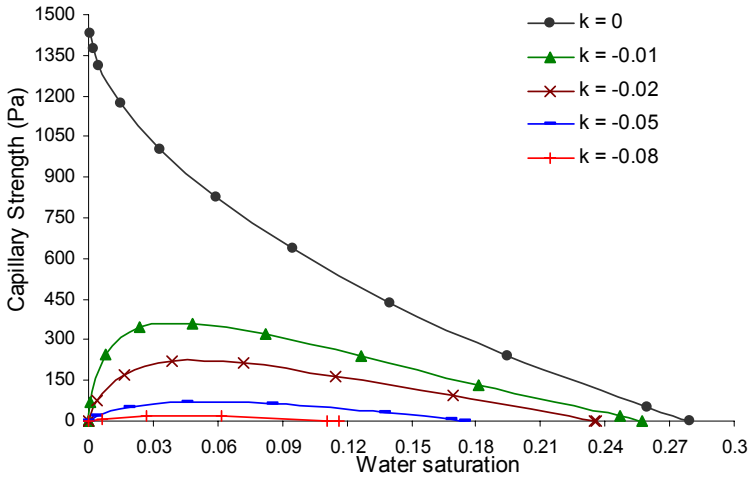

Fig.13: Variations of capillary strength (UCS) in squeezed state

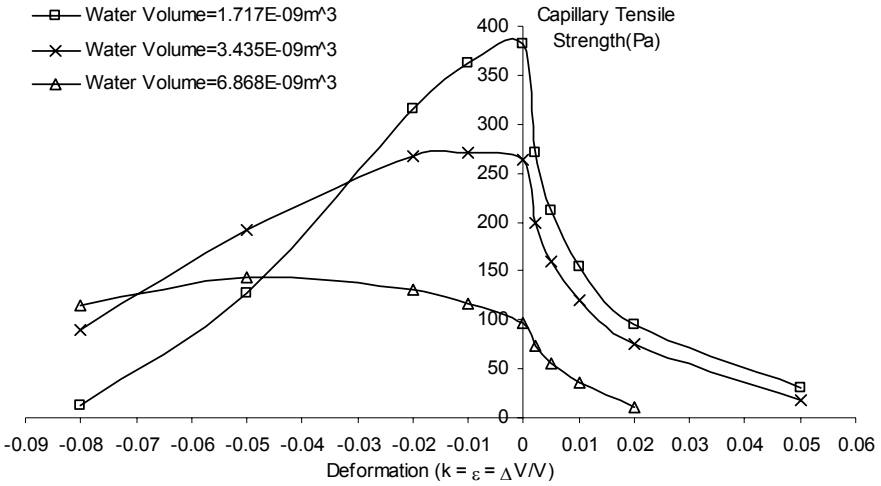

Fig.14: Behavior of capillary tensile strength with rock deformation

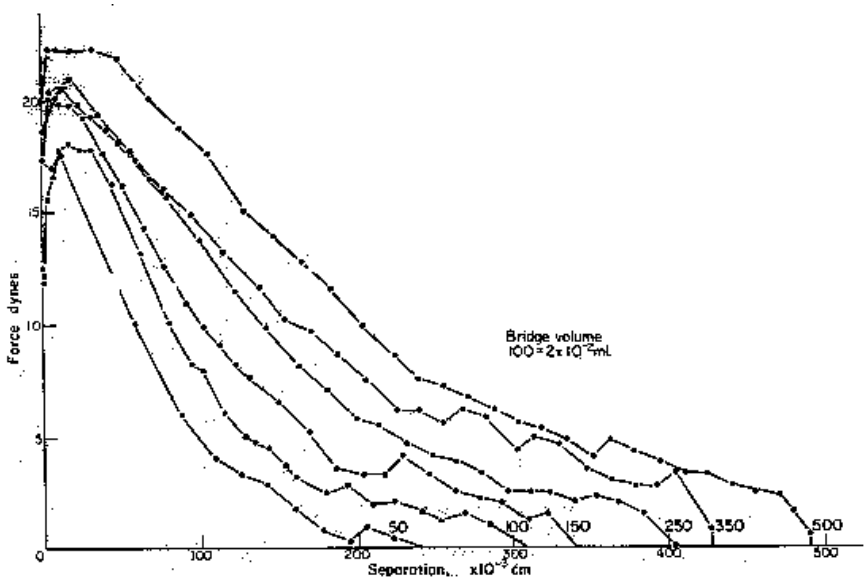

Fig.15: Capillary force variations with particle detachment at constant bridge volume (After Mason and Clark [25])